

X-ray, SEM, and DSC studies of ferroelectric $\text{Pb}_{1-x}\text{Ba}_x\text{TiO}_3$ ceramics

M. Roy · Praniti Dave · Shiv Kumar Barbar ·
Sumit Jangid · D. M. Phase · A. M. Awasthi

Received: 8 May 2009 / Accepted: 14 August 2009 / Published online: 19 September 2009
© Akadémiai Kiadó, Budapest, Hungary 2009

Abstract The polycrystalline ferroelectric compounds of general formula $\text{Pb}_{1-x}\text{Ba}_x\text{TiO}_3$ with $X = 0.00, 0.1, 0.2$ and 0.5 were prepared by high temperature solid-state reaction technique using high purity oxides and carbonates. The compounds formation was confirmed by X-ray diffraction and all the X-ray peaks were indexed with tetragonal structure of space group $P4mm$. Morphology and particle size of the compounds were obtained using scanning electron microscopy. Ferroelectric phase transition, enthalpy change, and specific heat of the compounds were obtained using modulated differential scanning calorimetry. It was observed that the phase transition temperature decreased linearly with the increase of substitution concentration.

Keywords Ferroelectrics · Heat capacity · Phase transition · SEM · X-ray diffraction

Introduction

Progress in materials development and characterization has led to the generation and identification of several novel, electronic, optoelectronic, and smart materials. Ferroelectric oxide-based ceramic materials are most promising for different electronic devices due to their high dielectric, piezoelectric, pyroelectric, and electro-optic constants as

well as the existence of hysteresis loop with bistable memory states [1–6]. In ABO_3 type perovskite ferroelectrics, A-cation occupies the corners and B-cation occupies the center position in the unit cell with oxygen ions at the centre of the faces. In this type of structure, A and B-cation sites may be substituted either fully or partially by the other homovalent or heterovalent cations [7–9]. It is possible to substitute more than one type of metal ions in the B-cation site for valence compensation [10, 11]. It is also observed that a combination of trivalent and pentavalent cation substitution on the B-site was favorable for the formation of the perovskite structure [12]. However, the large variations of composition are accompanied by changes in structure, which may have profound effect on the other physical properties of the materials. PbTiO_3 is one such perovskite type ferroelectric material having the following characteristics: transition temperature (T_c) = 763 K, tetragonality $c/a = 1.064$, and dielectric constant (K) = 200 at room temperature [13]. It has a large crystal anisotropy in the spontaneous polarization and because of this it is very difficult to prepare dense ceramics of pure PbTiO_3 [14, 15]. The combinations of divalent and pentavalent materials not only densify the material but also enhance the other physical characteristics. One such divalent additive is Ba, which takes the A-cation site in the perovskite structure. In the literature a large number of works have been reported on thin films and ceramics of pure and substituted PbTiO_3 [16–22] as well as either fully or partially substituted PbTiO_3 on B-cation site in the ceramic form [23]. But no systematic report appeared on the substitution of A-cation site in PbTiO_3 ceramic as we are reporting.

The present paper reports on the phase transition of $\text{Pb}_{1-x}\text{Ba}_x\text{TiO}_3$ ($X = 0.00, 0.1, 0.2, \text{ and } 0.5$) by differential scanning calorimetry (DSC) studies. In place of conventional DSC studies the phase transition is measured by

M. Roy (✉) · P. Dave · S. K. Barbar · S. Jangid
Department of Physics, M. L. Sukhadia University,
Udaipur 313002, Rajasthan, India
e-mail: mroy1959@yahoo.co.in

D. M. Phase · A. M. Awasthi
UGC-DAE-CSR, Indore, India

modulated differential scanning calorimetry (MDSC). In MDSC an additional sinusoidal thermal excitation is superimposed as if two experiments are running simultaneously. The linear heating rate provides the information about heat flow (enthalpy exchange, ΔH), whereas the sinusoidal heating rate provides the heat capacity (C_p) of the material under investigation. Therefore, MDSC gives more quantitative and accurate measurement of heat capacity as well as enthalpy change at the transition temperature. Not only this but complex transitions can also be analyzed more accurately and easily through MDSC.

Experimental

The polycrystalline samples of $\text{Pb}_{1-x}\text{Ba}_x\text{TiO}_3$ with $X = 0.00, 0.1, 0.2,$ and 0.5 have been prepared using the high purity chemicals PbO , BaCO_3 , and TiO_2 (99.9% pure obtained from Aldrich chemicals Co USA and CDH Bombay) by standard solid-state reaction technique. The stoichiometric amounts of these oxides and carbonates were mixed and milled for several hours and then calcined at 1073–1173 K for 24 h. The process of milling and calcinations was repeated for a number of times and finally cylindrical pellets were made after applying pressure around 498 MPa ($\sim 5 \text{ t/cm}^2$) in a hydraulic press. These pellets were sintered at $\sim 1423 \text{ K}$ for 4–6 h. The formation of the single phase compounds was confirmed by X-ray diffraction technique using the Rigaku X-ray diffractometer with Cu K_α radiation and nickel filter in a wide range of 2θ from 10° to 90° with a scanning rate of 2° per minute. The instrument was calibrated using the pure silicon sample provided with the instrument. The surface morphology as well as particle size was measured by scanning electron microscopy (SEM) using the JEOL, JSM-5600 SEM with different magnifications in back scattered mode. The particle size was also measured using the Scherrer equation $t = 0.9\lambda/\beta\cos\theta$ where λ is the wavelength of the radiation used, β is the full width at half maximum, and θ is the diffraction angle. The modulated DSC measurement was carried out on TA Instruments Model 2910 MDSC equipment from room temperature (RT) to 873 K in inert (N_2) atmosphere with a heating rate of 5 K/min and $\pm 0.75 \text{ K}$ modulations per 60 s.

Results and discussion

The X-ray powder diffraction patterns of $\text{Pb}_{1-x}\text{Ba}_x\text{TiO}_3$ with $X = 0.00, 0.1, 0.2,$ and 0.5 are shown in the Fig. 1. From the figure it is clear that the X-ray diagrams of the

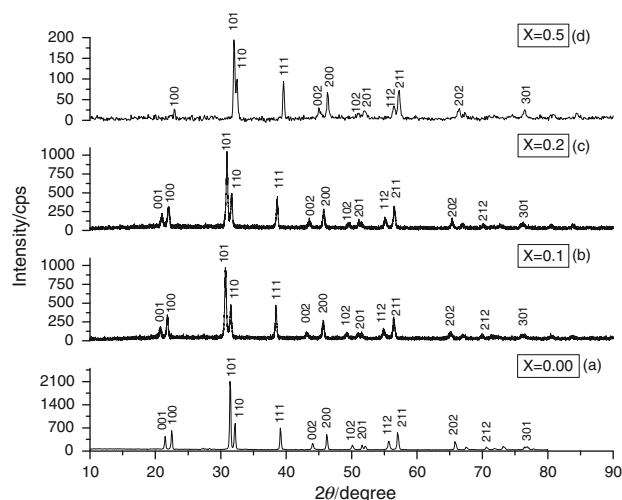


Fig. 1 X-ray diffractograms of $\text{Pb}_{1-x}\text{Ba}_x\text{TiO}_3$. $X = 0.00$ (a), $X = 0.1$ (b), $X = 0.2$ (c), and $X = 0.5$ (d)

substituted compounds are quite similar with that of the pure compound except $X = 0.5$ where 001 reflection peak is absent. It has also been observed that there is little shift in the peak positions of the substituted compounds, which are responsible for the corresponding minor change in the structural parameters. The interplanar spacings (d -values) obtained from the X-ray diagrams were used to calculate the cell parameters by least square refinement method using a standard computer program XRAYSCAN [24]. Comparison between observed (obtained from X-ray powder diagram) and calculated (based on refined cell parameters) d -values along with their Miller indices of the lattice planes (hkl values) show good agreement between them. To get a clear insight into the Ba-substitution effect on the lattice it is observed that the tetragonality ratio c/a is almost constant. The expansion and contraction of lattice parameters along a - and c -axes with the substitution of Ba^{2+} ion in place of Pb^{2+} ion is so small that the lattice distortion is least and c/a ratio remains invariant. Thus, X-ray analysis of all the samples indicated that the specimens are of single-phase perovskite type tetragonal structure with space group $P4mm$.

The morphology obtained from the SEM micrograph of the pure compound revealed that the particles are larger than the average particle size of the substituted compounds. Not only this, the distribution of the particles in the pure compound is not very regular nor compact and shows voids in between the grains. Due to this the pure compound even after proper sintering is often brittle showing its characteristic behavior consistent with the reported result [25]. The average particle size of the pure compound is around $5 \mu\text{m}$ (Fig. 2a). With the increase of substitution the

densification of the compounds increases and as the particle size reduces the density increases. Further increase in the concentration of foreign ions in the host cation site reduces the particle size more and more and densification increases. Not only that, the particle size becomes more and more spherical, showing the isotropic growth with an average particle size of less than $1\ \mu\text{m}$ (Fig. 2d), when the foreign ion concentration increased up to 0.5. With the increase of substitution the micrograph revealed that the

Table 1 Variation of T_c with concentration of Ba^{2+} ion in $\text{Pb}_{1-x}\text{Ba}_x\text{TiO}_3$ and its corresponding ΔH and particle size values

Ba^{2+} concentration/ In $\text{Pb}_{1-x}\text{Ba}_x\text{TiO}_3$	T_c/K	$\Delta H/\text{Jg}^{-1}$	Particle size/ μm
$X = 0.00$	761 ± 2	2.42	~ 5
$X = 0.1$	734	2.02	~ 2
$X = 0.2$	702	1.36	< 2
$X = 0.5$	596	0.67	< 1

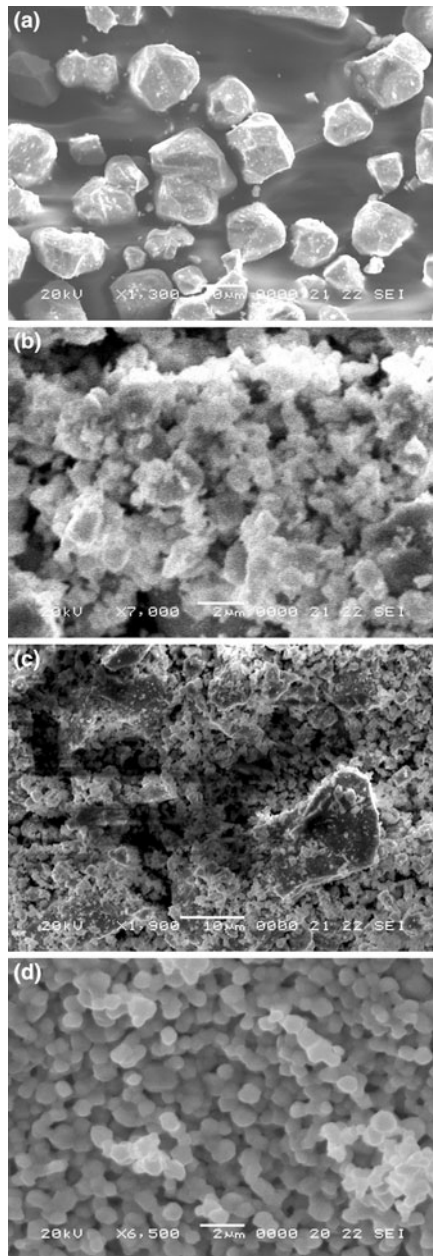


Fig. 2 SEM micrographs of $\text{Pb}_{1-x}\text{Ba}_x\text{TiO}_3$. $X = 0.00$ (a), $X = 0.1$ (b), $X = 0.2$ (c), and $X = 0.5$ (d)

morphology of the particles shows narrower size distribution with spherical and isotropic growth of particle with an average size that decreases with the increase of substitution concentration. The average particle size as determined from the SEM micrographs is in good agreement with that obtained from the X-ray diffraction by Scherrer formula and is shown in Table 1. The typical SEM micrographs for $X = 0.00, 0.1, 0.2,$ and 0.5 are shown in Fig. 2a–d.

The DSC curves of the pure and Ba^{2+} substituted PbTiO_3 compounds are shown in Fig. 3. From the figure it is clear that the pure PbTiO_3 compound (Fig. 3a) undergoes an endothermic ferroelectric phase transition at $T_c = 761 \pm 2\ \text{K}$ which is consistent with the reported value [25]. Due to modulated heating profile the MDSC provided a direct measurement of the specific heat of the material at T_c . Apart from the endothermic peak at T_c , no other peak/transition occurred in the measured temperature region. When the Ba^{2+} ion is substituted in the A-cation lattice site the T_c peak is shifted towards the lower value, with a decrease in specific heat value at T_c . With further increase of concentration the T_c decreases again. It is observed that the gradual increase in the concentration of Ba^{2+} ion on the A-cation site of the host lattice decreases the transition temperature and changes the specific heat as well. This gradual decrease of T_c and the corresponding change in the specific heat value with the increase of X -concentrations for $X = 0.00, 0.1, 0.2,$ and 0.5 have been shown in Fig. 3a–d and in Table 1. This change in T_c with the increase of substitution concentration of Ba^{2+} ion on removal of Pb^{2+} ion on A-cation site of the host lattice may be due to the difference in ionic size of Pb^{2+} and Ba^{2+} as discussed in our earlier paper [6] as well as their different thermal characteristics. This systematic change in T_c is consistent with our X-ray data and SEM micrographs. The plot of T_c versus the substitution concentration shows an inverse relation (Fig. 4). The decrease in T_c with the increase of substitution concentration has already been explained above in Fig. 3a–d. Hence Fig. 4 is self explanatory and need not require further explanation.

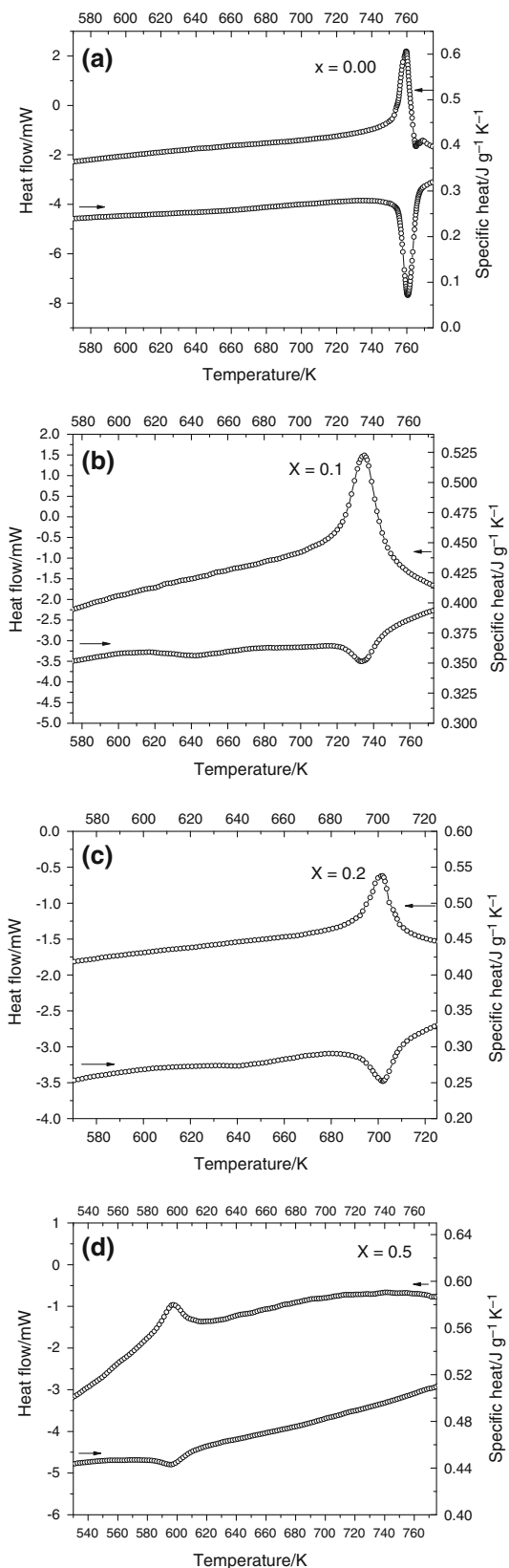


Fig. 3 Specific heat/heat flow versus temperature curve of $\text{Pb}_{1-x}\text{Ba}_x\text{TiO}_3$. $X = 0.00$ (a), $X = 0.1$ (b), $X = 0.2$ (c), and $X = 0.5$ (d)

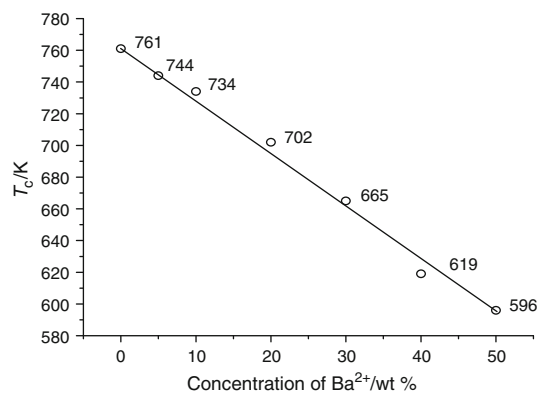


Fig. 4 Variation of T_c with the concentration of Ba^{2+} in $\text{Pb}_{1-x}\text{Ba}_x\text{TiO}_3$. $X = 0.00, 0.1, 0.2$, and 0.5 (also included $X = 0.05, 0.3$, and 0.4)

Conclusions

From the above studies it is concluded that the binding strength among the particles of the pure PbTiO_3 compound is so poor that the distribution of the particles become irregular and show voids in between the grains even after applying the proper sintering conditions of time and temperature. Hence pure compound shows very high value of $T_c \sim 763$ K. But with the gradual increase of the homo-valent isoelectronic cation substitution on A-cation site, the binding strength among the particles increases causing the reduction in particle size and hence enhanced density. Due to reduction in particle size the thermal stability of the material is increasing and transition temperature decreasing. Thus, we see that the substitution of isoelectronic foreign atom on the A-cation site of the host lattice, the material characteristics get improved and provide better results for eventual functionality.

Acknowledgements We are thankful to Mr. Suresh Bhardwaj and Mr. V. K. Ahire for their help in conducting the experiments.

References

1. Lines ME, Glass AM. Principle and applications of ferroelectrics and related materials. Clarendon: Oxford; 1979.
2. Damjanovic D. Ferroelectric, dielectric and piezoelectric properties of ferroelectric thin films and ceramics. Rep Prog Phys. 1998;61:1267–324.
3. Dey SK, Zuleeg R. Processing and parameters of sol-gel PZT thin-films for GaAs memory applications. Ferroelectrics. 1990;112: 309–19.
4. Takarama R, Tomita Y, Asvama J, Nomura K, Cawa HO. Pyroelectric infra red array sensors made of c-axis oriented Lamodified PbTiO_3 thin films. Sens Actuators A. 1990;22:508–12.
5. Sanches LE, Wu SY, Naik IK. Observations of ferroelectric polarization reversal in sol-gel processed very thin lead-zirconate-titanate films. J Appl Phys Lett. 1990;56:2399–401.

6. Roy M, Choudhary RNP, Acharya HN. Differential scanning calorimetric studies of ferroelectric rare molybdates. *Thermochim Acta*. 1989;145:11–7.
7. Radecka M, Rekas M. Microcalorimetry studies of phase transitions in $(\text{Ba}_x\text{Sr}_{1-x})\text{TiO}_3$. *J Therm Anal Calorim*. 2007;88:731–4.
8. Zaremba T. Thermoanalytical study of the synthesis of $\text{Na}_{0.5}\text{Bi}_{0.5}\text{TiO}_3$ ferroelectric. *J Therm Anal Calorim*. 2008;92:583–7.
9. Bernardi MIB, Antonelli E, Lourenco AB, Feitosa CAC, Maia LJQ, Hernandes AC. $\text{BaTi}_{1-x}\text{Zr}_x\text{O}_3$ nanopowders prepared by the modified Pechini method. *J Therm Anal Calorim*. 2007;87:725–30.
10. Roy-Chowdhury P, Shiralkar VP. Studies of some doped lead titanate ceramics. *Indian J Pure Appl Phys*. 1968;6:591–5.
11. Ikegami S, Ueda I, Nagata T. Electromechanical properties of PbTiO_3 ceramics containing La and Mn. *J Acoust Soc America*. 1971;50:1060–6.
12. Roy R. Multiple ions substitution in the perovskite lattice. *J Am Ceram Soc*. 1954;37:581–8.
13. Jain JD. Ferroelectric materials: trends and applications. *IETE Tech Rev*. 1985;2:238–47.
14. Ito Y, Takeuchi H, Jyomura S, Nagatsuma K, Ashida S. Temperature compensated PbTiO_3 ceramics for surface acoustic wave applications. *Appl Phys Lett*. 1979;35:595–7.
15. Kuwata J, Uchino K, Nomura S. Dielectric and piezoelectric properties of $0.91\text{Pb}(\text{Zn}_{1/3}\text{Nb}_{2/3})\text{O}_3$ - 0.09PbTiO_3 single crystals. *Jpn J Appl Phys*. 1982;21:1298–302.
16. Lee KB, Tirumala S, Desu SB. Highly c-axis oriented $\text{Pb}(\text{Zr},\text{Ti})\text{O}_3$ thin films grown on Ir electrode barrier and their electrical properties. *Appl Phys Lett*. 1999;74:1484–6.
17. Zhang ZG, Chu DP, McGregor BM, Migliorato P, Ohashi K, Hasegawa K, et al. Frequency dependence of the dielectric properties of La doped $\text{Pb}(\text{Zr}_{0.35}\text{Ti}_{0.65})\text{O}_3$ thin films. *Appl Phys Lett*. 2003;83:2892–4.
18. Fong DD, Kolpak AM, Eastman JA, Streiffer SK, Fuoss PH, Stephenson GB, et al. Stabilization of monodomain polarization in ultra thin PbTiO_3 films. *Phys Rev Lett*. 2006;96:127601–4.
19. Wang Y, Wang KF, Zhu C, Liu JM. Polarization fatigue of ferroelectric $\text{Pb}(\text{Zr}_{0.1}\text{Ti}_{0.9})\text{O}_3$ thin films: temperature dependence. *J Appl Phys* 2006;99:044109-1-6.
20. Poyato R, Lourdes Calzada M, Pardo L. $(\text{Pb},\text{La})\text{TiO}_3/(\text{Pb},\text{Ca})\text{-TiO}_3$ ferroelectric heterostructures for nonvolatile memories. *Appl Phys Lett*. 2005;86:042905-1-3.
21. Zorel HE Jr, Crespi MS, Ribeiro CA. Attainment of lead titanate through thermal decomposition of coprecipitated 8-hydroxyquinolate precursors. *J Therm Anal Calorim*. 2004;75:545–50.
22. Mesquita A, Bernardi MIB, Maia LJQ, Mastelaro VR. Synthesis and characterization of $\text{Pb}_{1-x}\text{La}_x\text{TiO}_3$ nanocrystalline powders. *J Therm Anal Calorim*. 2007;87:747–51.
23. Pelaiz-Barranco A, Marin-Franch P. Piezo-, pyro-, ferro-, and dielectric properties of ceramic/polymer composites obtained from two modifications of lead titanate. *J Appl Phys*. 2005;97:034104-1-5.
24. Hwang JS, Tien C. XRAYSCAN: an indexing program considering dense spurious peaks in an optimization method. *Chin J Phys*. 1996;34:47–57.
25. Jaffe B, Roth RS, Marzullo S. Properties of piezoelectric ceramics in the solid solution series lead titanate-lead zirconate-lead oxide: tin oxide and lead titanate-lead hafnate. *J Res Nat Bur Stand*. 1955;55:239–54.